2013 IEEE/RSJ International Conference on
Intelligent Robots and Systems (IROS)
November 3-7, 2013. Tokyo, Japan

Limit Cycle Walking on Ice

Fumihiko Asano[1], Yasunori Kikuchi[1] and Masahiro Shibata[1]

***Abstract*— This paper investigates modeling and control of a limit cycle walker that walks sliding on the ice. We introduce the model of an underactuated spoked walker for analysis and analyze the collision model on the assumption of sliding contact with the ground to identify the condition for achieving instantaneous exchange of the stance leg. We also develop the equation of motion incorporating dynamic friction in sliding contact. Numerical simulations show that the walker can generate stable walking gaits by applying a simple control of the torso.**

I. INTRODUCTION

Including passive dynamic walking [1], in modeling of limit cycle walking, it is commonly assumed that the end point of the stance leg is always in contact with the ground without sliding [2][3]. This implicitly supports that the contact point develops sufficient friction. On the ice, however, this assumption cannot hold. This paper then addresses two issues; one is identifying the condition for achieving instantaneous exchange of the stance leg and the other is generation of stable walking gaits on the ice. First, we introduce the model of an underactuated spoked walker with a torso that falls as a 1-DOF rigid body immediately prior to impact [4], and develop the inelastic collision model on the assumption that the walker is sliding at impact. We then identify the condition that the rear leg leaves the ground immediately after landing of the fore leg. Second, we develop the equation of motion incorporating dynamic friction in sliding contact and numerically test the possibility of stable gait generation on the ice. Numerical analysis of the gait properties show that there is an optimal friction coefficient for achieving the most efficient walking gait.

Bourgeot et al. discussed the variety of the post-impact motion of a dynamic walker that falls as a 1-DOF rigid body based on the concept of rocking block, and they divided the possible motion into four cases according to the relation between the pre-impact velocity and the post-impact one [5]. Font-Llangunes and Kövecses also discussed this issue and analyzed the post-impact state of a compass-like biped robot. They identified the condition for transition to double-limb support (DLS) based on the vertical velocity of the end-position of the rear leg [6]. In this paper, however, we take a different approach; we analytically derive the impulse vector which is derived as a zero-time integral of the impulsive forces at impact and examine the sign of each element to determine unilateral constraint [7]. Through mathematical investigations, we show that the result obtained is equivalent to those of the related works [5][6]. Furthermore, we numerically investigate the properties of the generated gait on the ice and show that there are the optimal solutions of friction coefficient for achieving the maximum walking speed.

[1]F. Asano, Y. Kikuchi and M. Shibata are with the School of Information Science, Japan Advanced Institute of Science and Technology, 1-1 Asahidai, Nomi, Ishikawa 923-1292, Japan {fasano,yasunori_kikuchi,masahiro.shibata} @jaist.ac.jp

II. COLLISION ANALYSIS

A. Underactuated Spoked Walker with Torso

Fig. 1 shows the model of an underactuated spoked walker which composed of a twelve-legged rimless wheel and a torso. Let m_1 [kg] and I_1 [kg·m^2] be the mass and inertia moment of the rimless wheel. Let m_2 [kg] and I_2 [kg·m^2] be those of the torso. The leg length or the radius of the rimless wheel is l [m]. The length of the torso is $2r$ [m] and this is connected to the rimless wheel at the central joint. This walker can exert a joint torque, u [N·m], between the stance leg and the torso. The torso functions as a reaction wheel for the RW; the stance leg can use the reaction torque for propulsion.

B. Inelastic Collision Model

Let $\boldsymbol{q} = \begin{bmatrix} x & z & \theta_1 & \theta_2 \end{bmatrix}^{\mathrm{T}}$ be the generalized coordinate vector. Here, (x, z) is the position of the stance-leg end, θ_1 is the stance-leg angle with respect to vertical, and θ_2 is the torso angle with respect to horizontal. The inelastic collision of the fore leg (the next stance leg) with the ground is then modeled as

$$\boldsymbol{M}(\boldsymbol{q})\dot{\boldsymbol{q}}^+ = \boldsymbol{M}(\boldsymbol{q})\dot{\boldsymbol{q}}^- + \boldsymbol{J}_I(\boldsymbol{q})^{\mathrm{T}}\boldsymbol{\lambda}_I, \tag{1}$$

where the superscripts "$-$" and "$+$" stand for immediately before and immediately after impact. Note that $\boldsymbol{q}$ in Eq. (1) is equal to $\boldsymbol{q}^- = \boldsymbol{q}^+$. $\boldsymbol{M}(\boldsymbol{q}) \in \mathbb{R}^{4\times 4}$ is the inertia matrix and is detailed as

$$\boldsymbol{M}(\boldsymbol{q}) = \begin{bmatrix} m_t & 0 & m_t l\cos\theta_1 & 0 \\ 0 & m_t & -m_t l\sin\theta_1 & 0 \\ m_t l\cos\theta_1 & -m_t l\sin\theta_1 & m_t l^2 + I_1 & 0 \\ 0 & 0 & 0 & I_2 \end{bmatrix}, \tag{2}$$

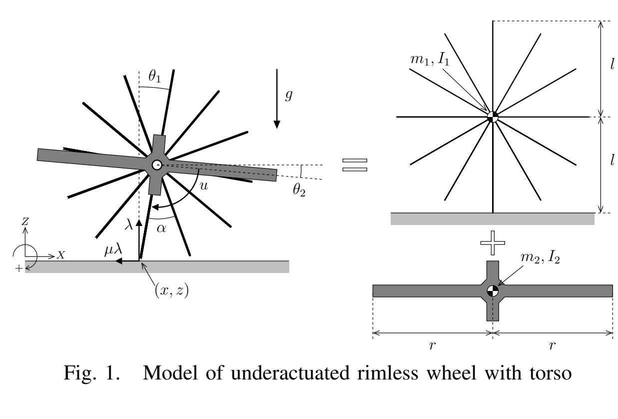

Fig. 1. Model of underactuated rimless wheel with torso

where $m_t := m_1 + m_2$ [kg] is the total mass. The size of the Jacobian matrix, $\boldsymbol{J}_I(\boldsymbol{q})$, is non-unique and changes according to the condition for velocity constraint at impact. In the following, we describe the conditions in detail.

C. Condition for Instantaneous Stance-leg Exchange

First, we analytically derive the condition for achieving instantaneous stance-leg exchange by assuming that the motion transitions to DLS after impact.

If we assume that the fore leg slides at impact, that is, the end-point is not constrained in the X-direction, the only velocity constraint condition is given by

$$\frac{\mathrm{d}}{\mathrm{d}t}\left(z + l\cos\theta_1^- - l\cos(\alpha - \theta_1^-)\right)^+ = 0, \tag{3}$$

where $\theta_1^- = \alpha/2$ [rad].

We generally assume that the contact point between the stance-leg end and the hard ground develops sufficient friction and that the end point does not slide steadily or the constraint condition of $\dot{x}^+ = 0$ always holds. In this case, the walking motion consists of single-limb support (SLS) and instantaneous DLS for stance-leg exchange. On the ice, however, this is not true and we must develop the Jacobian matrix, $\boldsymbol{J}_I(\boldsymbol{q})$, in Eq. (1) accordingly. The lack of $\dot{x}^+ = 0$ implies that a redundant DOF is created. We therefore have to concern about the possible emergence of DLS motion after impact [7][8]. Transition to DLS motion implies that the walker continues sliding without rotating. In the following, we discuss the problem of how to determine the post-impact motion, SLS or DLS, through mathematical analysis of the impulse.

If we assume that the rear leg does not leave the ground immediately after landing of the fore leg or maintains contact with the ground, the following condition must hold.

$$\dot{z}^+ = 0 \tag{4}$$

In addition, in this paper we assume that the torso is mechanically locked to the RW at impact. This means that the walker falls down as a 1-DOF rigid body immediately before impact. This velocity constraint condition is then specified as

$$\dot{\theta}_1^+ - \dot{\theta}_2^+ = 0. \tag{5}$$

By summarizing Eqs. (3), (4), and (5), we get

$$\boldsymbol{J}_I(\boldsymbol{q})\dot{\boldsymbol{q}}^+ = \boldsymbol{0}_{3\times 1} \tag{6}$$

$$\boldsymbol{J}_I(\boldsymbol{q}) = \begin{bmatrix} 0 & 1 & -l\sin\theta_1^- + l\sin(\theta_1^- - \alpha) & 0 \\ 0 & 1 & 0 & 0 \\ 0 & 0 & 1 & -1 \end{bmatrix}. \tag{7}$$

Following Eqs. (1) and (6), the impulse vector, $\boldsymbol{\lambda}_I \in \mathbb{R}^3$, can be solved as

$$\boldsymbol{\lambda}_I = -\boldsymbol{X}_I(\boldsymbol{q})^{-1}\boldsymbol{J}_I(\boldsymbol{q})\dot{\boldsymbol{q}}^- = \begin{bmatrix} \frac{2I_t + m_t l^2(1-\cos\alpha)}{4l\sin\frac{\alpha}{2}} \\ -\frac{2I_t - m_t l^2(1-\cos\alpha)}{4l\sin\frac{\alpha}{2}} \\ I_2 \end{bmatrix}\dot{\theta}_1^-, \tag{8}$$

where $\boldsymbol{X}_I(\boldsymbol{q}) := \boldsymbol{J}_I(\boldsymbol{q})\boldsymbol{M}(\boldsymbol{q})^{-1}\boldsymbol{J}_I(\boldsymbol{q})^{\mathrm{T}}$ and $I_t := I_1 + I_2$ [kg·m^2] is the total inertia moment. By substituting $\boldsymbol{\lambda}_I$ of Eq. (8) into Eq. (1), the velocity vector immediately after impact, $\dot{\boldsymbol{q}}^+$, is derived as

$$\dot{\boldsymbol{q}}^+ = \left(\boldsymbol{I}_4 - \boldsymbol{M}(\boldsymbol{q})^{-1}\boldsymbol{J}_I(\boldsymbol{q})^{\mathrm{T}}\boldsymbol{X}_I(\boldsymbol{q})^{-1}\boldsymbol{J}_I(\boldsymbol{q})\right)\dot{\boldsymbol{q}}^- \tag{9}$$

$$= \begin{bmatrix} \dot{x}^- + l\dot{\theta}_1^-\cos\frac{\alpha}{2} \\ 0 \\ 0 \\ 0 \end{bmatrix}. \tag{10}$$

The result of $\dot{\theta}_1^+ = \dot{\theta}_2^+ = 0$ implies that the walker begins to slide in the X-direction maintaining DLS.

The first element in Eq. (8) represents the impulse (zero-time integral of impulsive force at impact) in Z-direction at the end of the fore leg, and the second element represents that of the rear leg. It is obvious that the first element is always positive. The second element becomes positive only if the following inequality holds.

$$m_t l^2(1-\cos\alpha) \geq 2I_t \tag{11}$$

If Eq. (11) holds, the motion transitions to DLS.

The left-hand side in Eq. (11) converges to zero if $\alpha \to 0$. Small α increases the potential of instantaneous stance-leg exchange. Let us consider a numerical example in the following. By choosing the parameters as listed in Table I, the value of the left-hand side in Eq. (11) becomes 0.402, whereas that of the right-hand side becomes 3.0. We then conclude that DLS motion does not emerge after impact. The right-hand value in Eq. (11) is the total inertia moment, so the value is large implies that the rotational energy immediately before impact is large. The resultant SLS motion after impact in this case is therefore convincing.

In the case that the rear leg leaves the ground immediately after impact, the condition of Eq. (4) is not necessary and $\boldsymbol{J}_I(\boldsymbol{q}) \in \mathbb{R}^{2\times 3}$ then becomes

$$\boldsymbol{J}_I(\boldsymbol{q}) = \begin{bmatrix} 0 & 1 & -l\sin\theta_1^- + l\sin(\theta_1^- - \alpha) & 0 \\ 0 & 0 & 1 & -1 \end{bmatrix}. \tag{12}$$

By using this, $\boldsymbol{\lambda}_I \in \mathbb{R}^2$ is derived as

$$\boldsymbol{\lambda}_I = \frac{4m_t l\sin\frac{\alpha}{2}\dot{\theta}_1^-}{2I_t + m_t l^2(1-\cos\alpha)}\begin{bmatrix} I_t \\ I_2 l\sin\frac{\alpha}{2} \end{bmatrix}. \tag{13}$$

It is obvious that all the elements of $\boldsymbol{\lambda}_I$ are positive if and only if $\dot{\theta}_1^- > 0$. By substituting Eq. (13) into Eq. (9), we can derive $\dot{\boldsymbol{q}}^+$ and its elements are detailed as follows.

$$\dot{x}^+ = \dot{x}^- + \frac{2m_t l^3\sin\frac{\alpha}{2}\sin\alpha}{2I_t + m_t l^2(1-\cos\alpha)}\dot{\theta}_1^- \tag{14}$$

$$\dot{z}^+ = \frac{2\left(2I_t - m_t l^2(1-\cos\alpha)\right)l\sin\frac{\alpha}{2}}{2I_t + m_t l^2(1-\cos\alpha)}\dot{\theta}_1^- \tag{15}$$

$$\dot{\theta}_1^+ = \dot{\theta}_2^+ = \frac{2I_t - m_t l^2(1-\cos\alpha)}{2I_t + m_t l^2(1-\cos\alpha)}\dot{\theta}_1^- \tag{16}$$

TABLE I
PHYSICAL PARAMETERS FOR WALKING MODEL

m_1	2.0	kg	α	30	deg
m_2	1.0	kg	$I_1 = m_1\left(\frac{l}{2}\right)^2$	0.5	kg·m^2
l	1.0	m			
r	1.0	m	$I_2 = m_2 r^2$	1.0	kg·m^2

Note that $\dot{x}^+$ and $\dot{z}^+$ in the above equations are the velocities at the end-position of the rear leg immediately after impact. Eq. (15) implies that $\dot{z}^+$ becomes positive if the condition of Eq. (11) holds. This means that the following two conditions are equivalent.

(C1) The velocity of the end-position of the rear leg, $\dot{z}^+$, is negative.

(C2) The impulse in vertical direction of the rear leg is positive.

(C1) is the condition Bourgeot et al. and Font-Llagunes and Kövecses derived [5][6]. (C2) is that one of the authors derived [7].

The transition rules for the positional coordinates are described in the following. At the start of walking, we set the end-position of the stance leg (x, z) to $(0, 0)$. At every impact, we reset x to

$$x^+ = x^- + 2l\sin\frac{\alpha}{2}. \tag{17}$$

It is obvious that $z^\pm = 0$ holds. The angular position of the stance leg, θ_1, should be reset to

$$\theta_1^+ = \theta_1^- - \alpha = -\frac{\alpha}{2}. \tag{18}$$

Also $\theta_2^\pm = 0$ must hold on the assumption that the output following control is achieved as described later.

III. EQUATION OF MOTION AND CONTROLLER DESIGN

A. Equation of Motion

The equation of motion corresponding to the generalized coordinate vector, $\boldsymbol{q}$, becomes

$$\boldsymbol{M}(\boldsymbol{q})\ddot{\boldsymbol{q}} + \boldsymbol{h}(\boldsymbol{q}, \dot{\boldsymbol{q}}) = \boldsymbol{S}u + \boldsymbol{J}^{\mathrm{T}}\lambda + \boldsymbol{J}_\mu^{\mathrm{T}}\lambda, \tag{19}$$

where the first term of the right-hand side is the control input vector, the second term is the vector of the holonomic constraint force between the stance-leg end and the floor, and the third term is the vector of the dynamic friction force. In the left-hand side, $\boldsymbol{M}(\boldsymbol{q})$ is the same as Eq. (2) and the vectors $\boldsymbol{h}(\boldsymbol{q}, \dot{\boldsymbol{q}}) \in \mathbb{R}^4$ and $\boldsymbol{S} \in \mathbb{R}^4$ are detailed as follows.

$$\boldsymbol{h}(\boldsymbol{q}, \dot{\boldsymbol{q}}) = \begin{bmatrix} -m_t l\dot{\theta}_1^2 \sin\theta_1 \\ m_t\left(g - l\dot{\theta}_1^2\cos\theta_1\right) \\ -m_t g l \sin\theta_1 \\ 0 \end{bmatrix}, \quad \boldsymbol{S} = \begin{bmatrix} 0 \\ 0 \\ 1 \\ -1 \end{bmatrix} \tag{20}$$

As previously mentioned, the stance-leg exchange is instantaneous and the continuous motion is always SLS. The condition for the holonomic constraint during the stance phase is then given by

$$\dot{z} = \boldsymbol{J}\dot{\boldsymbol{q}} = 0, \quad \boldsymbol{J} = \begin{bmatrix} 0 & 1 & 0 & 0 \end{bmatrix}. \tag{21}$$

By solving Eqs. (19) and (21) for λ, we get

$$\lambda = -\frac{\boldsymbol{J}\boldsymbol{M}(\boldsymbol{q})^{-1}\left(\boldsymbol{S}u - \boldsymbol{h}(\boldsymbol{q}, \dot{\boldsymbol{q}})\right)}{\boldsymbol{J}\boldsymbol{M}(\boldsymbol{q})^{-1}\hat{\boldsymbol{J}}^{\mathrm{T}}} \tag{22}$$

$$= \frac{2m_t\left(I_1\left(g - l\dot{\theta}_1^2\cos\theta_1\right) - ul\sin\theta_1\right)}{2I_1 + m_t l^2\left(1 - \cos(2\theta_1) - \mu\sin(2\theta_1)\right)}. \tag{23}$$

By observing the sign of λ, we can check the unilateral constraint.

The dynamic friction force in sliding contact is given by $\mu\lambda$ [N]. Here, μ is the coefficient of dynamic friction and this includes the direction of the friction force. The Jacobian, $\boldsymbol{J}_\mu$, is then determined as $\boldsymbol{J}_\mu = \begin{bmatrix} \mu & 0 & 0 & 0 \end{bmatrix}$. μ should be, for example,

$$\mu(\dot{\boldsymbol{q}}) = \mu_0\mathrm{sign}(\dot{x}), \tag{24}$$

where μ_0 is a positive constant. There is no standard value of μ_0 because measured value of it changes in accordance with temperature and ice quality [9][10]. We then set small values less than 1.0 for simple modeling. For avoiding chattering, we consider an approximation of Eq. (24) around $\dot{x} = 0$ as follows.

$$\mu(\dot{\boldsymbol{q}}) = -\mu_0\tanh(c\dot{x}) \tag{25}$$

Where c is a positive constant. Following Eqs. (19) and (21), we can eliminate λ in Eq. (19) and arrange it as follows.

$$\boldsymbol{M}(\boldsymbol{q})\ddot{\boldsymbol{q}} \;=\; \boldsymbol{Y}(\boldsymbol{q}, \dot{\boldsymbol{q}})\left(\boldsymbol{S}u - \boldsymbol{h}(\boldsymbol{q}, \dot{\boldsymbol{q}})\right) \tag{26}$$

$$\boldsymbol{Y}(\boldsymbol{q}, \dot{\boldsymbol{q}}) \;:=\; \boldsymbol{I}_4 - \hat{\boldsymbol{J}}(\dot{\boldsymbol{q}})^{\mathrm{T}}\left(\boldsymbol{J}\boldsymbol{M}(\boldsymbol{q})^{-1}\hat{\boldsymbol{J}}(\dot{\boldsymbol{q}})^{\mathrm{T}}\right)^{-1} \times\boldsymbol{J}\boldsymbol{M}(\boldsymbol{q})^{-1} \tag{27}$$

$$\hat{\boldsymbol{J}}(\dot{\boldsymbol{q}}) \;:=\; \boldsymbol{J} + \boldsymbol{J}_\mu(\dot{\boldsymbol{q}}) \tag{28}$$

B. Input-Output Linearization and Control Input

Let $y := \theta_1 - \theta_2 = \boldsymbol{S}^{\mathrm{T}}\boldsymbol{q}$ be the control output and consider tracking control of y to $y_{\mathrm{d}}(t)$. The second-order derivative of y with respect to time becomes

$$\ddot{y} = \boldsymbol{S}^{\mathrm{T}}\ddot{\boldsymbol{q}} = \boldsymbol{S}^{\mathrm{T}}\boldsymbol{M}(\boldsymbol{q})^{-1}\boldsymbol{Y}(\boldsymbol{q}, \dot{\boldsymbol{q}})\left(\boldsymbol{S}u - \boldsymbol{h}(\boldsymbol{q}, \dot{\boldsymbol{q}})\right). \tag{29}$$

Then we can consider the control input for achieving $y \to y_{\mathrm{d}}(t)$ as follows.

$$u \;=\; A(\boldsymbol{q}, \dot{\boldsymbol{q}})^{-1}\left(v(t) + B(\boldsymbol{q}, \dot{\boldsymbol{q}})\right) \tag{30}$$

$$v(t) \;=\; \ddot{y}_{\mathrm{d}}(t) + K_D\left(\dot{y}_{\mathrm{d}}(t) - \dot{y}\right) + K_P\left(y_{\mathrm{d}}(t) - y\right) \tag{31}$$

The scalar functions $A(\boldsymbol{q}, \dot{\boldsymbol{q}})$ and $B(\boldsymbol{q}, \dot{\boldsymbol{q}})$ are defined as

$$A(\boldsymbol{q}, \dot{\boldsymbol{q}}) \;:=\; \boldsymbol{S}^{\mathrm{T}}\boldsymbol{M}(\boldsymbol{q})^{-1}\boldsymbol{Y}(\boldsymbol{q}, \dot{\boldsymbol{q}})\boldsymbol{S},$$

$$B(\boldsymbol{q}, \dot{\boldsymbol{q}}) \;:=\; \boldsymbol{S}^{\mathrm{T}}\boldsymbol{M}(\boldsymbol{q})^{-1}\boldsymbol{Y}(\boldsymbol{q}, \dot{\boldsymbol{q}})\boldsymbol{h}(\boldsymbol{q}, \dot{\boldsymbol{q}}).$$

K_P and K_D are PD gains and are positive constants. y is, however, exactly controlled to follow $y_{\mathrm{d}}(t)$ and PD feedback is not necessary because $y^+ = -\alpha/2$ and $\dot{y}^+ = 0$ hold. To smoothly control y from $-\alpha/2$ to $\alpha/2$ during the stance phases, we introduce $y_{\mathrm{d}}(t)$ as the following 5-order time-dependent function.

$$y_{\mathrm{d}}(t) = \begin{cases} \dfrac{6\alpha}{T_{\mathrm{set}}^5}t^5 - \dfrac{15\alpha}{T_{\mathrm{set}}^4}t^4 + \dfrac{10\alpha}{T_{\mathrm{set}}^3}t^3 - \dfrac{\alpha}{2} & (0 \le t < T_{\mathrm{set}}) \\ \dfrac{\alpha}{2} & (t \ge T_{\mathrm{set}}) \end{cases}$$

Here, note that the time variable, t, is reset to zero at every impact. $y_{\mathrm{d}}(t)$ satisfies the following boundary conditions.

$$y_{\mathrm{d}}(0^+) = -\frac{\alpha}{2}, \quad \dot{y}_{\mathrm{d}}(0^+) = 0, \quad \ddot{y}_{\mathrm{d}}(0^+) = 0$$

$$y_{\mathrm{d}}(T_{\mathrm{set}}) = \frac{\alpha}{2}, \quad \dot{y}_{\mathrm{d}}(T_{\mathrm{set}}) = 0, \quad \ddot{y}_{\mathrm{d}}(T_{\mathrm{set}}) = 0$$

We assume that the output following control is completed by the next impact.

IV. GAIT ANALYSIS

A. Typical Walking Gait and Stability

We chose the initial condition as

$$\boldsymbol{q}(0) = \begin{bmatrix} 0 & 0 & -\alpha/2 & 0 \end{bmatrix}^{\mathrm{T}}, \quad \dot{\boldsymbol{q}}(0) = \begin{bmatrix} 0 & 0 & V_0 & V_0 \end{bmatrix}^{\mathrm{T}}, \tag{32}$$

where V_0 [rad/s] is the initial angular velocity. Fig. 2 shows the simulation results of level dynamic walking where $T_{\mathrm{set}} = 0.30$ [s], $\mu_0 = 0$ and $V_0 = 0.80$ [rad/s]. We can see that a stable walking gait is successfully generated on the completely frictionless surface. From Fig. 2 (a), we can also see that x decreases or the contact point slides backward during the stance phases.

Fig. 3 shows the evolutions of the gait descriptors for three values of V_0 with respect to the step number. Here, (a) is the step period, and (b) is the walking speed. From Fig. 3 (a), we can see that the step periods converge to the steady one at a fast convergent speed. From Fig. 3 (b), however, we can see that the walking speeds are kept different constant values according to the initial angular velocities. We can conclude that the generated gaits are stable but the limit cycles are not unique. The steady walking speed monotonically increases as the initial angular velocity increases.

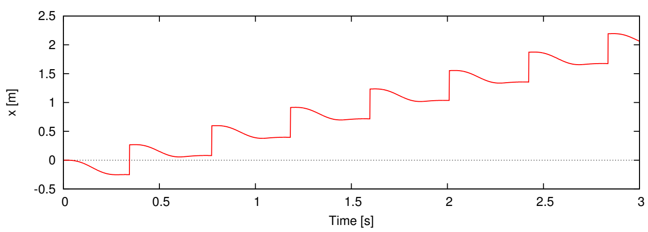

(a) x

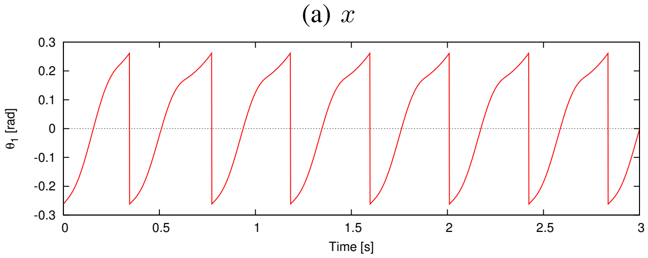

(b) θ_1

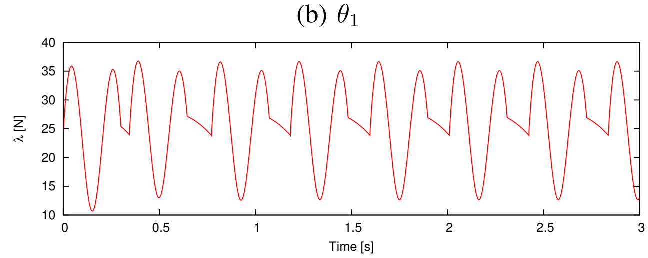

(c) λ

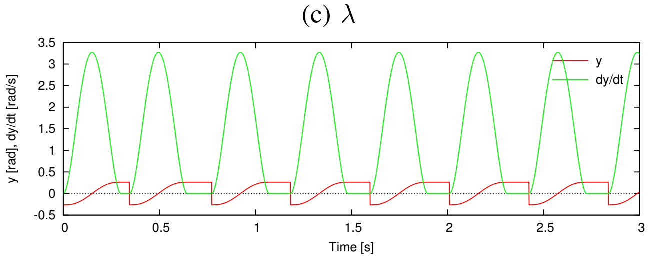

(d) y and $\dot{y}$

Fig. 2. Simulation results of dynamic walking on ice where $T_{\mathrm{set}} = 0.30$ [s] and $\mu_0 = 0$

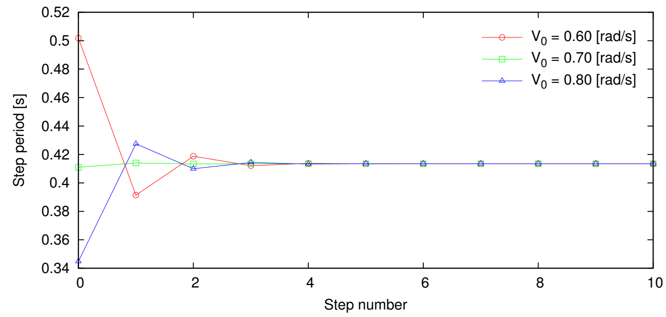

(a) Step period

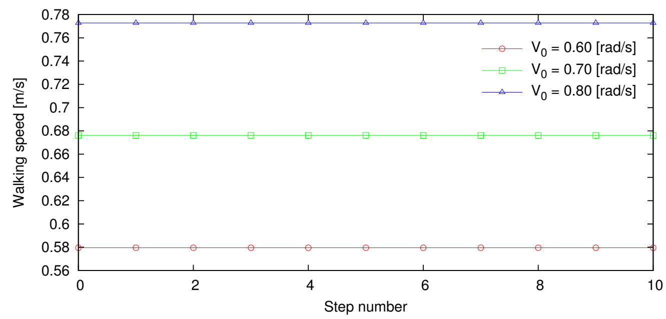

(b) Walking speed

Fig. 3. Evolutions of gait descriptors where $\mu_0 = 0$

Fig. 4 shows the simulation results of level dynamic walking where $\mu_0 = 0.4$. The initial conditions were chosen as the same in Eq. (32). From the results, we can see that a stable gait is successfully generated. Fig. 4 (a) supports that the contact point, x, slides forward during the stance phases, that is, the walker in this case can move forward more smoothly than the previous case. The sliding contact enables the walker to increase the forward momentum and to thrust against the floor. The step length is also increased by the effect of sliding.

B. Gait Properties

Before gait analysis, we define the gait descriptors for evaluating the efficiency of the generated walking gaits.

The average walking speed is defined as

$$V = \frac{\Delta x}{T}.$$

Here, T [s] is the step period. Δx [m] is the step length defined as the change in x from an instant immediately after impact to the next, i.e. is defined as

$$\Delta x := \int_{0^+}^{T^-} \dot{x}\ \mathrm{d}t + 2l \sin\frac{\alpha}{2}. \tag{33}$$

The energy efficiency is evaluated in terms of the specific resistance (SR) which is a dimensionless quantity and is defined as

$$\mathrm{SR} := \frac{p}{m_t g V}.$$

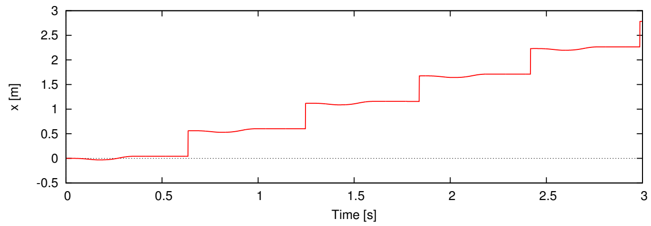

(a) x

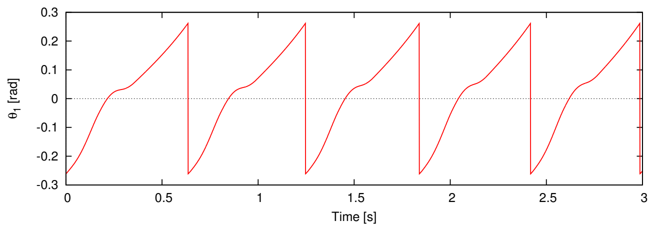

(b) θ_1

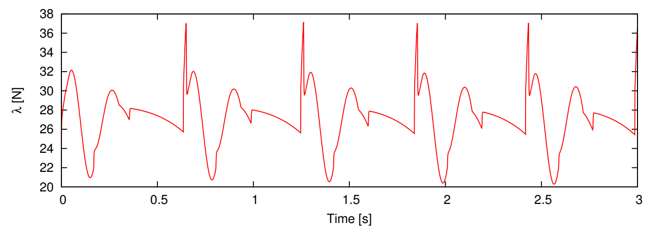

(c) λ

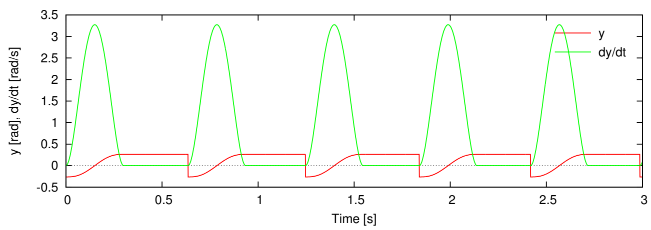

(d) y and $\dot{y}$

Fig. 4. Simulation results of dynamic walking on ice where $T_{\text{set}} = 0.30$ [s] and $\mu_0 = 0.4$

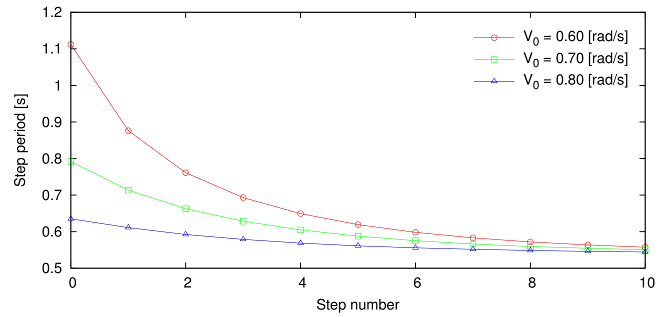

(a) Step period

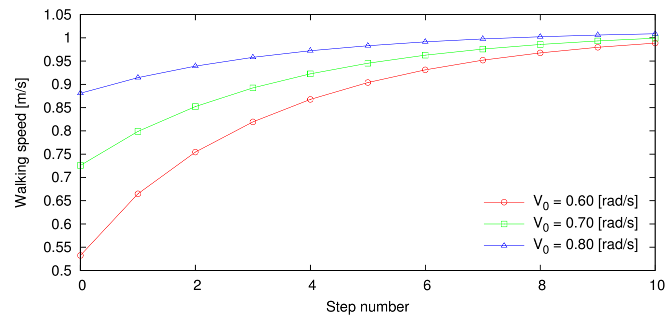

(b) Walking speed

Fig. 5. Evolutions of gait descriptors where $\mu_0 = 0.2$

Here, p [J/s] is the average input power defined by

$$p := \frac{1}{T} \int_{0^+}^{T^-} |\dot{y}u| \, \mathrm{d}t.$$

We performed numerical simulations by taking the following procedures.

(P1) Set μ_0 to zero.

(P2) Set the initial conditions to those in Eq. (32) where $V_0 = 0.80$ [rad/s].

(P3) Run the walking simulation for over 100 [s], and save the gait descriptors and the steady state variables immediately after impact.

(P4) Increase μ_0 by 0.01 and rerun the walking simulation by using the state variables saved in (P3) as the new initial conditions.

(P5) Repeat from (P3) to (P4) until $\mu_0 = 1.0$.

Fig. 6 shows the gait descriptors for three values of T_{set} with respect to μ_0. Here, (a) is the step period T, (b) the step length Δx, (c) the walking speed V, and (d) the specific resistance. In the cases where $T_{\text{set}} = 0.3$ and 0.4 [s], stable gaits were generated for all μ_0. Where $T_{\text{set}} = 0.2$ [s], stable gaits could not be generated with small values of μ_0 because the ground reaction force, λ, became negative during the stance phases. The small T_{set} generates a great deal of joint torque, and this induces a substantial change in vertical acceleration.

Except the step period, there are significant differences between the gait descriptors where $\mu_0 = 0$ and those where $\mu_0 = 0.01$. This fact implies that the gait efficiency dramatically improves if there is the slightest effect of dynamic friction. In contrast, the gait efficiency can be improved flexibly by adding external energy sources after converging a steady gait where $\mu_0 = 0$.

From Fig. 6 (b), we can see that the step lengths in the cases where $T_{\text{set}} = 0.30$ and 0.40 [s] converge to the steady ones and that there are the ranges of μ_0 where the step lengths are more than the steady ones. In these ranges, the walker slides forward during the stance phases and the step length becomes longer as shown in Fig. 4 (a). As μ_0 increases more, however, the motion during the stance phases becomes equivalent to that in the absence of sliding due to big friction. The first term of the right-hand side in Eq. (33) therefore converges to zero. To confirm this, we plotted

$$2l \sin \frac{\alpha}{2} = 0.517638 \text{ [m]}$$

in the figure. Also the step length where $T_{\text{set}} = 0.20$ would converge to this value if μ_0 increases more.

Fig. 6 (c) and (d) show that there is a unique μ_0 that maximizes the walking speed or minimizes the SR in each case. The walking speed is maximized in the case that the contact point, x, slides forward well during the stance phases and the step period is reasonably short. The values of μ_0 are close to each other but are different. We must conclude that

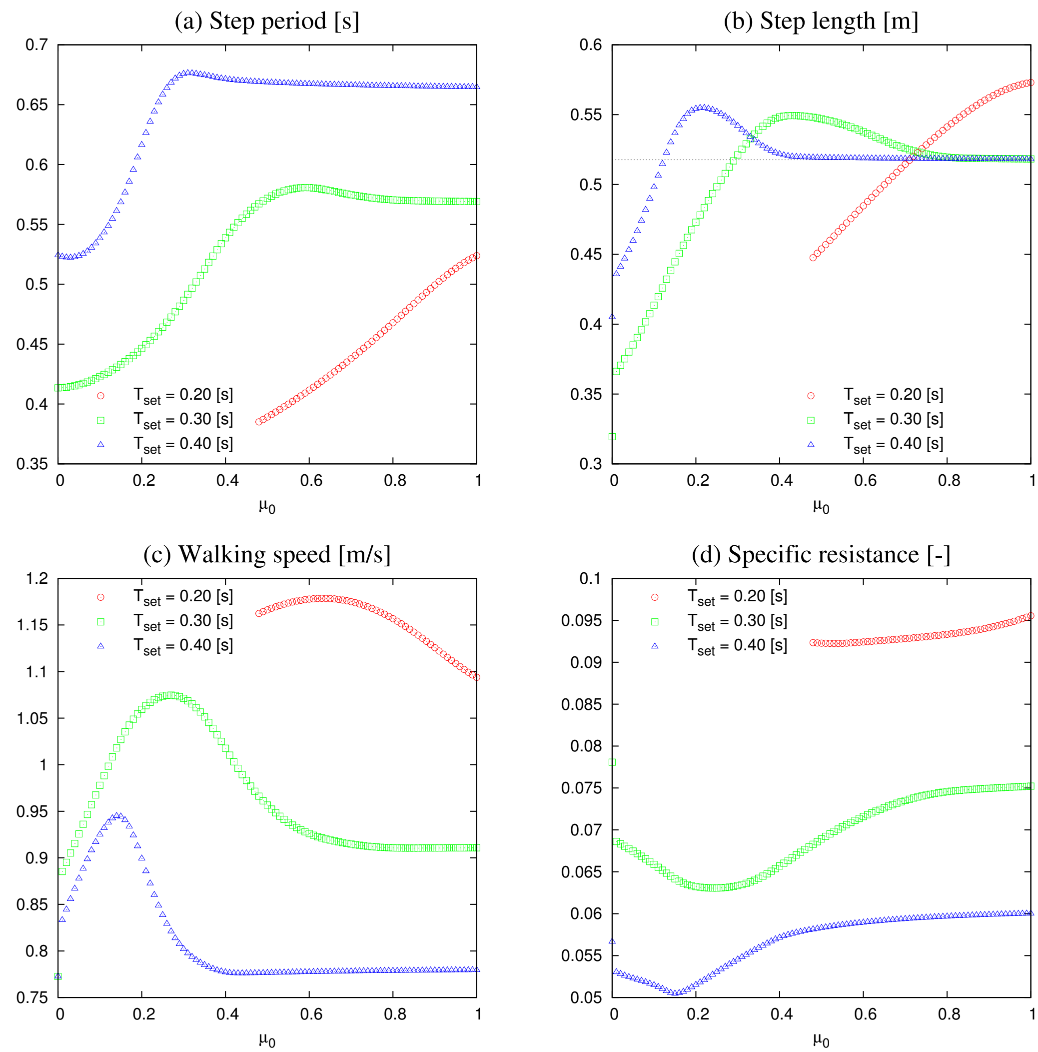

Fig. 6. Gait descriptors for three values of $T_{\rm set}$ with respect to μ_0

the optimal solution for μ_0 depends on the criterion.

V. CONCLUSION AND FUTURE WORK

In this paper, we discussed modeling and control of limit cycle walking incorporating the effect of dynamic friction in sliding contact. Through mathematical analysis, we identified the condition for achieving instantaneous stance-leg exchange. Numerical simulations showed that the optimal solutions of the friction coefficient to the walking speed and SR are different.

In the future, we should discuss more realistic model of dynamic friction and extend mathematical analysis to various walking models. Application to stabilizing control and efficient gait generation utilizing the frictional effect is also left as a future work.

REFERENCES

[1] T. McGeer, "Passive dynamic walking," *Int. J. of Robotics Research*, Vol. 9, No. 2, pp. 62–82, 1990.

[2] M. J. Coleman, A. Chatterjee and A. Ruina, "Motions of a rimless spoked wheel: a simple three-dimensional system with impacts," *Dynamics and Stability of Systems*, Vol. 12, Iss. 3, pp. 139–159, 1997.

[3] F. Asano, "Stability principle underlying passive dynamic walking of rimless wheel," *Proc. of the IEEE Int. Conf. on Control Applications*, pp. 1039–1044, 2012.

[4] F. Asano and X. Xiao, "Output deadbeat control approaches to fast convergent gait generation of underactuated spoked walker," *Proc. of the IEEE/SICE Int. Symp. on System Integration (SII)*, pp. 265–270, 2012.

[5] J.-M. Bourgeot, C. Canudas-de-Wit and B. Brogliato, "Impact shaping for double support walk: from the rocking block to the biped robot," *Proc. of the 8th Int. Conf. on Climbing and Walking Robots and the Support Technologies for Mobile Robots*, pp. 509–516, 2005.

[6] J. M. Font-Llagunes and J. Kövecses, "Dynamics and energetics of a class of bipedal walking systems," *Mechanism and Machine Theory*, Vol. 44, Iss. 11, pp. 1999–2019, 2009.

[7] F. Asano and M. Ohshima, "Emergence of measurable period of double-limb support in limit cycle walking with knees," *Proc. of the IEEE Int. Conf. on Control Applications*, pp. 1045–1050, 2012.

[8] F. Asano and J. Kawamoto, "Passive dynamic walking of viscoelastic-legged rimless wheel," *Proc. of the IEEE Int. Conf. on Robotics and Automation*, pp. 2331–2336, 2012.

[9] F. P. Bowden, "Friction on snow and ice," *Proc. of the Royal Society of London, A*, Vol. 217, Iss. 1131, pp. 462–478, 1953.

[10] D. Kuroiwa, "The kinetic friction on snow and ice," *J. of Graciology*, Vol. 19, No. 81, pp. 141–152, 1977.